Quad Band Planar Monopole Antenna with Polarization Diversity for FSS and SAR Application

Reshmi Dhara

Abstract Here, a simple, planar monopole antenna with polarization diversity for quad band application using a single feed mechanism has been reported. The design antenna which is proposed here involves two L-shaped radiators with two asymmetric cross slots within it creating mutual coupling to attain dual circularly polarized (CP) bands. To generate quad impedance bandwidth (IBW), defective ground plane is utilized on the bottom portion on the substrate. The antenna which is proposed covered the quad simulated IBs that are from 3.631–4.167 GHz (535.6 MHz, $f_{rc1} = 3.9$ GHz, 13.73%), 6.542–8.494 GHz (1951.8 MHz, $f_{rc2} = 7.52$ GHz, 25.96%), 8.859–10.253 GHz (1134.3 MHz, $f_{rc3} = 9.56$ GHz, 14.59%) and 10.8494–beyond 15 GHz (4150.6 MHz, $f_{rc4} = 12.92$ GHz, 32.19%), respectively. The simulated dual ARBWs span over 3.865–4.069 GHz (203.7 MHz, $f_{cp1} = 3.97$ GHz, 5.14%) within 1st IB and 8.888–9.785 GHz (897.3 MHz, $f_{cp2} = 9.34$ GHz, 9.6%) within 3rd IB. The simulated peak gain between 2.2 and 6.01dBi span throughout IBW region makes the dual CP bands appropriate for some part of S- and X-band, particularly fixed-satellite service (FSS) and synthetic aperture radar (SAR) applications.

Keywords Quad band · Polarization diversity · Axial ratio bandwidth · Impedance bandwidth · FSS · SAR

1 Introduction

Recently, multiband antennas with polarization diversity have satisfied multiple necessities of many devices in wireless communication systems. In personal global position system (GPS) appliances and mobile, antennas through omnidirectional radiation are particularly suitable. On the other hand, several communication devices,

R. Dhara (✉)
Department of Electronics and Communication Engineering, National Institute of Technology Sikkim, South Sikkim, Gangtok, Ravangla PIN 737 139, India
e-mail: reshmidhara@nitsikkim.ac.in

R. Dhavse et al. (eds.), *Emerging Technology Trends in Electronics, Communication and Networking*, Lecture Notes in Electrical Engineering 952,
https://doi.org/10.1007/978-981-19-6737-5_8

different satellite communication systems, and antennas having unidirectional radiation patterns are growing by means of an integral technology. To generate vertically/horizontally omnidirectional dual-polarized radiation, it is needed to superimpose two radiation from a monopole antenna which is vertically polarized and a loop antenna which is horizontally polarized. Now in communication system where the astronomical research is the main attention, several uses communication devices are essential as a substitute to single communication typical device. As a consequence of the striking characteristics like lower footprint, simpler geometry, and lighter in weight, planar monopole antennas help as an utmost suitable practice. This is known to all that a conventional monopole antenna in longitudinal direction creates linearly polarized (LP) wave. But the foremost drawbacks of linear polarized wave expected at dual-band process are lower sensitivity and multipath fading towards the positioning between the antenna which are transmitting and receiving, lower mobility, and like that [1–3]. This might be overwhelmed to a great scope for antennas which consume the circular polarization. Henceforth, dual-band antennas by means of two different frequency bands instantaneously functioning dual circular polarization (left-hand circular polarization (LHCP) and right-hand circular polarization (RHCP)) are significantly widespread compared to dual-band antennas with two quadrature (vertically/horizontally) linear polarizations. The requirement of multiple antennas decreases due to using a multiband antenna by means of dual-polarization features. The CP antenna is very attractive for many wireless systems as no strict alignment is required among antenna which is transmitting and receiving and encountering interference. To fulfil these necessities of multiband antenna presentation together with linear and circular polarization, various methodologies have been used by many researchers [4–8].

Inspired by the aforementioned whole thing, a simple quad band monopole antenna with LHCP in 1st band, LP in 2nd, LHCP in 3rd, and LP in 4th bands is proposed in this paper. The proposed design can support 3.631–4.167 GHz, 6.542–8.494 GHz, 8.859–10.253 GHz, and 10.8494 beyond 15 GHz. To design a quad antenna, it has been appropriately improved in method so that it can sustain together with linear and circular polarizations.

An actual good reflection coefficient, widespread ARBW and dependable radiation features are gained for the implemented antenna. It became apparent that the implemented antenna is simple and makes available for wider LP and CP frequency bands.

This paper is represented like Sect. 2: Design Procedure of Antenna; Sect. 3: Simulation Justifications and Discussions; and lastly Sect. 4: Conclusion.

2 Design Procedure of Antenna

An antenna with Quad band with polarization diversity can gratify the several purposes for changed device; they are generally used in wireless communication systems [9].

The designed antenna simulated structures are depicted in Fig. 1a and b. The size of the microstrip antenna is 70 × 60mm^2 (70 × 60 mm^2, i.e. 1.378 × 1.181 $\lambda_g{}^2$, λ_g = guided wavelength at 3.6 GHz). Commonly available, low-cost workable FR4-epoxy substrate thickness of 1.6 mm, having effective permittivity εr = 4.4 and tanδ = 0.02 (loss tangent), is utilized to simulate the implemented antenna. Comprehensive optimal dimensions are recorded in Table 1.

The progress steps of the implemented antenna are represented in Fig. 2. Figure 3a and b demonstrates the reflection coefficient and axial ratio bandwidth progress plots of the designed antenna. First, Antenna.1 is designed at a resonating frequency 3.6 GHz using a rectangular radiator and a ground plane rectangular in size on the reverse side of the substrate for FSS application. Here, a centre feed microstrip line is utilized to feed the antenna. But the IBW is very poor at this frequency and also got a CP in the higher frequency region (12.8 GHz). To progress the IBW and to satisfy the multiband characteristics by using the same dimension of the antenna, it is needed to create additional current paths. For that reason, two L-shaped radiators are used by modifying the rectangular-shaped radiator. The gap between two radiators creates a

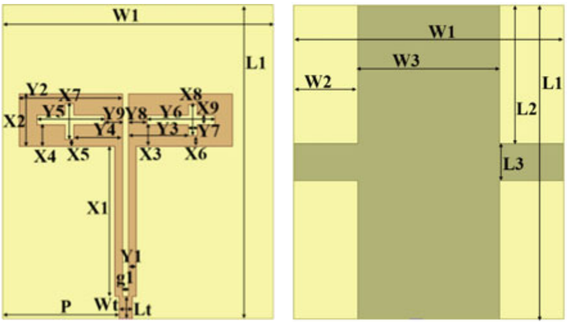

(a) Top View (b) Bottom View

Fig. 1 Dimension of proposed antenna

Table 1 Proposed antenna optimal dimension

Parameter	Value (mm)	Parameter	Value (mm)	Parameter	Value (mm)
L1	70	L2	30.9	L3	8.2
W1	60	W2	14.3	W3	31.4
Lt	5	Wt	3	g1	1.4
X1	33.5	X2	11.7	X3	4.8
X4	4.8	X5	1.7	X6	2.0
X7	7.8	X8	7.0	X9	2.1
Y1	1.7	Y2	23	Y3	13.2
Y4	10.8	Y5 = Y6	15	Y7	2.0
Y8 = Y9	4	P	25.8	h	1.6

coupling effect due to generation of capacitance between them. This gap creates additional current path that increases IBW in addition to improve ARBW performance compared to earlier stage. To improve ARBW performance more, also an asymmetric feed [8] is used in this step. Better impedance matching network can be performed by this feeding structure. Here, using defective ground plane improves the IBW performance of the implemented antenna [9]. But this Antenna.2 generates only a small CP (13.8 GHz) band. In the next stage to improve ARBW more <3dB, two slots asymmetric in size [10–12] are edged from two L-shaped radiator gives Antenna.3. These two slots generate two CP bands resonating at frequency 3.97 GHz and 9.34 GHz, respectively. These asymmetric slots [10, 11] create two orthogonal electric fields with equal amplitude at these two-resonating frequencies. This Antenna.3 helps to achieve quad impedance band resonating at 3.9 GHz, 7.52 GHz, 9.56 GHz, and >12.92 GHz, respectively. Since it satisfied our purpose, it definite to select finalized this design and analysed its performance.

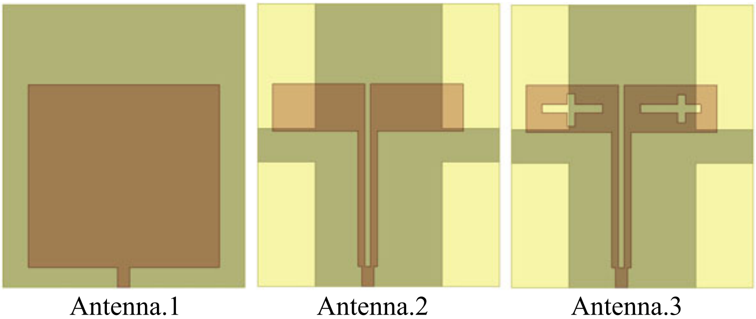

Fig. 2 Improvement of implemented antenna

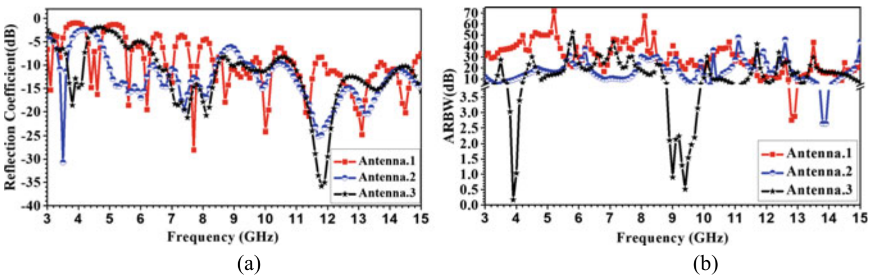

Fig. 3 Evaluation of **a** reflection coefficient (dB) and **b** ARBW (dB) for antennas. 1–3

3 Simulation Justifications and Discussions

To design the antenna, use Ansys Electronics Desktop 2020 R1 simulation software. The designed antenna enclosed the quad simulated IBW ranged from 3.631–4.167 GHz (535.6 MHz, $f_{rc1} = 3.9$ GHz, 13.73%), 6.542–8.494 GHz (1951.8 MHz, $f_{rc2} = 7.52$ GHz, 25.96%), 8.859–10.253 GHz (1134.3 MHz, $f_{rc3} = 9.56$ GHz, 14.59%), and 10.8494–beyond 15 GHz (4150.6 MHz, $f_{rc4} = 12.92$ GHz, 32.19%) is depicted in Fig. 4a.

Figure 4b also depicts the simulated ARBW of the implemented antenna**.** The simulated dual ARBWs span over 3.865–4.069 GHz (203.7 MHz, $f_{cp1} = 3.97$ GHz, 5.14%) within 1st IB and 8.888–9.785 GHz (897.3 MHz, $f_{cp2} = 9.34$ GHz, 9.6%) within 3rd IB.

Figure 4b, simulated input impedance, is depicting at 50Ω microstrip feed line for the real (resistance) and imaginary (reactance) parts. Within the matching of IBs is fine because the resistance part of the impedance is closer to 50Ω, and the reactance part is closer to 0Ω.

From Fig. 4c, using Smith chart, one can see that on resonance frequency 3.7, 3.9, 7.5, 9.6, 12.92, and 15.0 GHz the normalized impedance (Z11) values are close to 1, whereas the complex reflection coefficient magnitude (Γ) values are also very small. So above values depict that best matching can occur on resonance frequencies because real part of Z11 approaches to 50Ω and imaginary part tends to 0Ω. Also,

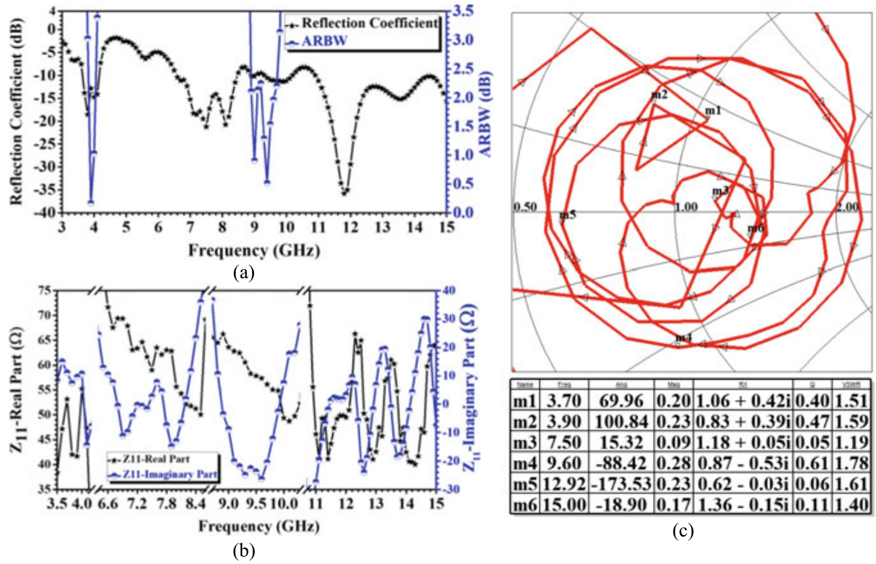

m1	3.70	69.96	0.20	1.06 + 0.42i	0.40	1.51
m2	3.90	100.84	0.23	0.83 + 0.39i	0.47	1.59
m3	7.50	15.32	0.09	1.18 + 0.05i	0.05	1.19
m4	9.60	-88.42	0.28	0.87 - 0.53i	0.61	1.78
m5	12.92	-173.53	0.23	0.62 - 0.03i	0.06	1.61
m6	15.00	-18.90	0.17	1.36 - 0.15i	0.11	1.40

Fig. 4 **a** Simulated reflection coefficient and ARBW curves comparisons, **b** simulated impedance (real and imaginary) vs. frequency curves, **c** results of the effect of complex reflection coefficient (Γ), normalized input impedance (Z11), Q-factor, and VSWR using Smith chart for the implemented antenna

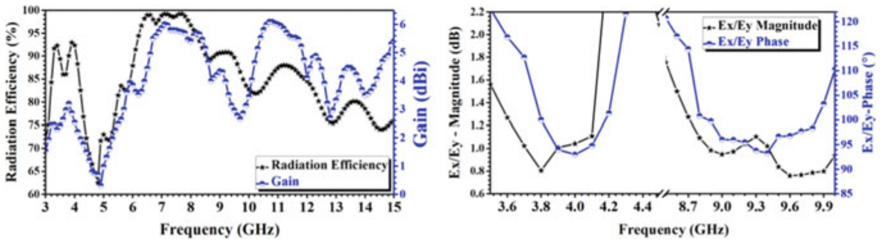

(a) (b)

Fig. 5 Proposed antenna **a** radiation efficiency and gain, **b** E_X/E_Y—magnitude and E_X/E_Y—phase plot versus frequency

VSWR value on those frequencies is also <2. The Q-value on those lower resonating frequencies in addition to higher resonating frequencies is also very small. That signifies widest IBW can occur due to small Q-factor. From this Smith chart, it is also clear that the graph rotates four times nearly equal to kick point (SWR = 1) which proves quad impedance bands are generated by using the same structure.

Figure 5a represents the radiation efficiency curve. The ranges of radiation efficiencies are between 74 and 99% for the quad IBs. The maximum efficiency is 99.17% at 7.1 GHz. Figure 5a also depicts the peak gains respecting frequency. The gain is within 2.20–6.01 dBi for quad IBs, and the peak gain is maximum 6.01 dBi at 7.1 GHz.

Figure 5b depicts the Ex/Ey magnitude is closely equal to 1 or 0 dB within the dual CP bands, and the difference of phase among them is also nearly 90°. That demonstrates that the dual bands gratify CP conditions [13].

Well-defined LHCP and RHCP are detected in Fig. 6a, c and b, d which illustrate at $f_{cp1} = 3.97$ GHz and $f_{cp2} = 9.34$ GHz resonating frequencies, the radiation patterns for $\varphi = 0°$ (XZ) and $\varphi = 90°$ (YZ) plane. At broadside direction on two CP resonating frequencies, the radiations observed are LHCP, whereas the polarization (co and cross) difference is 32.47 dBi and 22.57 dBi, correspondingly. Because of the asymmetric inset feeding radiator, the distribution of current is productive, due to that reason radiation is somewhat slanting from its broadside direction.

To understanding the generation of the dual CP modes at 3.97 and 9.34 GHz, a general studies are depicted in Figs. 7a and b. The normalized currents distribution from the below figures is observed that at four separate time moments (wherever T is the total time period for one cycle), dual CP modes could be accomplished at $f_{cp1} = 3.97$ GHz and $f_{cp2} = 9.34$ GHz which are LHCP.

The simulated axial ratio beam width at $f_{cp1} = 3.97$ and $f_{cp2} = 9.34$ GHz is plotted versus θ° in Fig. 8a and b. The simulated results at f_{cp1} the implemented antenna has a 3 dB axial ratio beam width with respect to vertical θ angle of about 17° at XZ ($\varphi = 0°$) plane and 89° at YZ ($\varphi = 90°$) plane. So, at broadside direction, the difference between co- and cross-plane for simulated 3 dB AR beam width is 72° at $f_{cp1} = 3.97$ GHz. Similarly, at f_{cp2}, the implemented antenna has a 3 dB axial ratio beam width over vertical θ angle of around 5° at XZ ($\varphi = 0°$) plane also 35° at YZ ($\varphi =$

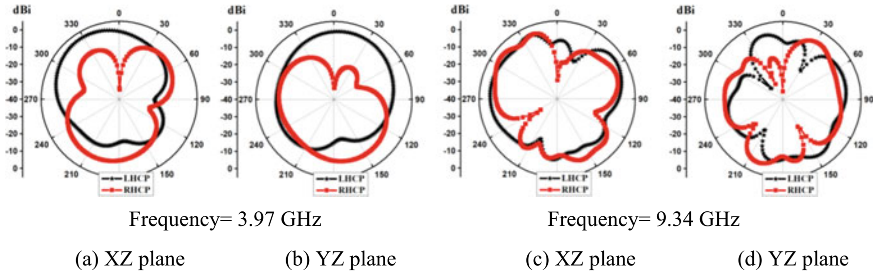

Fig. 6 Radiation patterns for (LHCP and RHCP) in the **a**, **c** XZ (φ = 0°) and **b**, **d** YZ (φ = 90°) planes

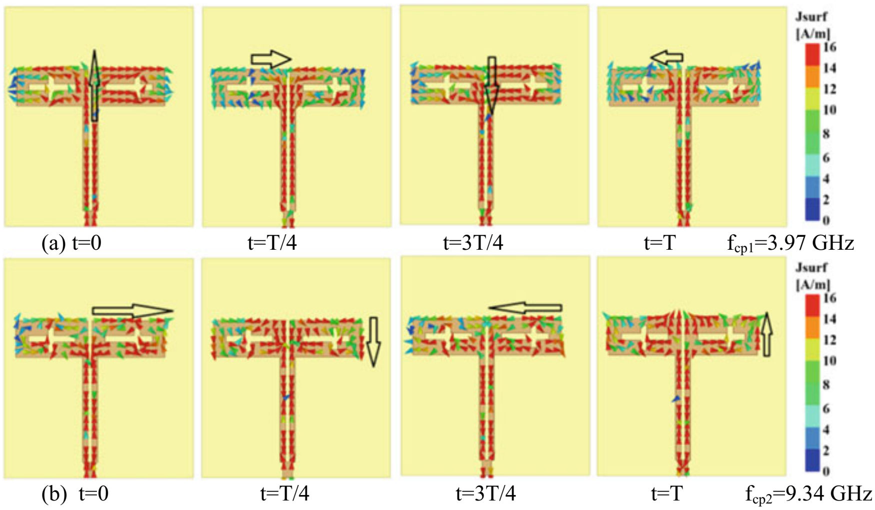

Fig. 7 Simulated current distribution at $f_{cp1} = 3.97$ and at $f_{cp2} = 9.34$ GHz

90°) plane. So, at broadside direction, the difference between co- and cross-plane for simulated 3 dB AR beam width is 30° at $f_{cp2} = 9.34$ GHz (Table 2).

4 Conclusion

A quad band antenna with polarization diversity characteristics bandwidth showing LHCP in 1st IB, LP in 2nd IB, LHCP in 3rd IB, and LP in 4th IB is comprehended by employing changes in ground plane and asymmetric feeding system of two L-shaped planar monopole antenna with two asymmetric cross-shaped slots. The proposed antenna (size 70 × 60 mm^2, i.e. 1.378 × 1.181 λ_g^2, λ_g = guided wavelength at 3.6 GHz) gives quad IBWs are 13.97, 25.96, 14.59, and 32.19% resonating at 3.9,

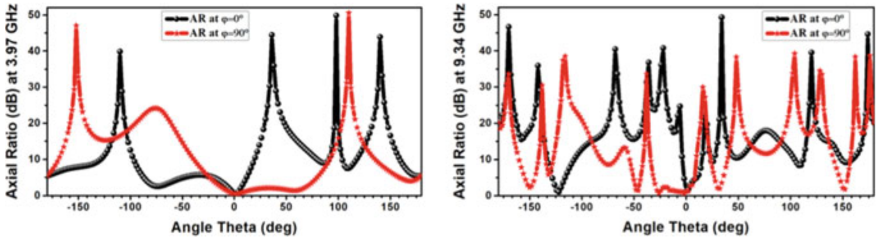

(a) (b)

Fig. 8 Axial ratio beam width versus θ° at XZ plane (φ = 0°) and YZ plane (φ = 90°) **c** f_{cp1} = 3.94 GHz, **b** f_{cp2} = 9.34 GHz for the proposed antenna

Table 2 Comparative study through related multiband antennas and proposed antenna

Ref. (year)	Polarization	IBW (%), f_{rc} (GHz)	ARBW (%), f_c (GHz)
4 (2011)	RHCP; LP	74; 39, 2.725; 7.15	16, 2.35
5 (2017)	RHCP; LP	3.93; 29.45, 5.845; 8.08	2.57, 5.84
6 (2019)	LP; LHCP	20.57; 68.74, 2.43; 7.39	18.5
7 (2020)	RHCP; LP	30.43; 14.94, 4.6; 8.1	27.89
8 (2021)	LP; RHCP	10.66; 61.18, 6.19; 10.445	41.41; 4.85, 9.105; 11.96
Proposed antenna	LHCP, LP, LHCP, LP	13.73; 25.96; 14.59; 32.19, 3.9, 7.52, 9.56, 12.92	5.14; 9.6, 3.97, 9.34

7.52, 9.56, and 12.92 GHz, respectively. The dual CP bands of this antenna can support S- and X-band specially FSS and SAR applications in a single device.

References

1. Toh BY, Cahill R, Fusco VF (2003) Understanding and measuring circular polarization. IEEE Trans Educ 46(3):313–318. https://doi.org/10.1109/TE.2003.813519
2. Yu D, Gong SX, Xu Y, Wan YT (2015) Dual-band dual-polarized circular microstrip patch antenna with the curved slots on the ground. Prog Electromagnet Res 51:27–31. https://doi.org/10.2528/PIERL14112004
3. Langston WL, Jackson DR (2004) Impedance, axial-ratio, and receive-power bandwidths of microstrip antennas. IEEE Trans Antennas Propag 52(10):2769–2774
4. Bao XL, Ammann MJ (2011) Wideband dual-frequency dual-polarized dipole-like antenna. IEEE Antennas Wirel Propag Lett 10:831–834. https://doi.org/10.1109/LAWP.2011.2164609

5. Ding K, Gao C, Wu Y, Qu D, Zhang B, Wang Y (2017) Dual-band and dual-polarized antenna with endfire radiation. IET Microwaves Antennas Propag 11(13):1823–1828. https://doi.org/10.1049/iet-map.2017.0124
6. Bag B, Biswas P, Biswas S, Sarkar PP (2019) Wide-bandwidth multifrequency circularly polarized monopole antenna for wireless communication applications. Int J RF Microwave Comput Aided Eng 29(3):e21631. https://doi.org/10.1002/mmce.21631
7. Madaka KCR, Muthusamy P Mode investigation of parasitic annular ring loaded dual band coplanar waveguide antenna with polarization diversity characteristics. Int J RF Microwave Comput-Aided Eng, pp e22119. https://doi.org/10.1002/mmce.22119
8. Dhara R (2021) A compact dual band dual polarized monopole antenna with enhanced bandwidth for C, X, and Ku band applications. Prog Electromagnet Res Lett 96:65–72. https://doi.org/10.2528/PIERL20121903
9. Dhara R, Jana SK, Mitra M (2020) Tri-band circularly polarized monopole antenna for wireless communication application. Radioelectron Commun Syst 63(4):213–222. https://doi.org/10.3103/S0735272720040044
10. Singh AK, Patil S, Kanaujia BK, Pandey VK (2020) A novel printed circularly polarized asymmetric wide slot antenna for digital cellular system. Microw Opt Technol Lett 62(3):1438–1447. https://doi.org/10.1002/mop.32177
11. Ellis MS, Effah FB, Ahmed AR, Kponyo JJ, Nourinia J, Ghobadi C, Mohammadi B (2020) Asymmetric circularly polarized open-slot antenna. Int J RF Microwave Comput Aided Eng 30(5):e22141. https://doi.org/10.1002/mmce.22141
12. Dhara R, Yadav S, Sharma MM, Jana SK, Govil MC (2021) A circularly polarized quad-band annular ring antenna with asymmetric ground plane using theory of characteristic modes. Prog Electromagnet Res 100:51–68. https://doi.org/10.2528/PIERM20102006
13. Dhara R, Mitra M (2020) A triple-band circularly polarized annular ring antenna with asymmetric ground plane for wireless applications. Eng Reports 2(4): e12150. https://doi.org/10.1002/eng2.12150